

CIRCULARLY POLARIZED PERIODIC LEAKY-WAVE ANTENNA BASED ON A COAXIAL LINE WITH HELICAL SLOT

ALEXANDRU ALOMAN¹, MIGUEL POVEDA-GARCIA², IOAN NICOLAESCU¹, FLORIN POPESCU¹, LAURENȚIU BUZINCU¹

Keywords: Leaky-wave antennas; Circular polarization; Frequency-scanned; Helical slot; Periodic leaky-wave antenna (LWA); Satellite communications.

A novel coaxial-line-based helical leaky-wave antenna (LWA) with circular polarization (CP) is presented in this work. The CP is achieved thanks to a helical-shaped slot edged on the outer conductor of the coaxial line that allows for controlled radiation when the fundamental TEM mode of the coaxial line is fed. Thus, a periodic-like LWA is formed with frequency-scanning of a conical beam and suppressed open stopband achieved thanks to the continuous radiation along the helical slot. This way, the radiation efficiency can be kept high in a wide scanning range. A prototype has been designed and manufactured for validation with beam scanning from -90° to 12° in the 8-16 GHz frequency range. The efficiency is above 75 % in almost all this frequency band with a simulated axial ratio below 3 dB, showing proper CP performance.

1. INTRODUCTION

CIRCULAR polarization (CP) is a key feature of antenna systems towards traditional satellite communications (SatCom) since it is required to overcome Faraday's ionospheric polarization rotation [1]. Moreover, in modern CubeSat constellations [2–4], antennas capable of radiating with CP are preferred since the relative orientation between the satellites is variable. In addition, for wideband communications, it is necessary to increase frequency. Consequently, the path loss is increased, and high gain is needed. For this, antennas based on reflectors have been widely used in SatCom, due to their high gain. The classical solution for the feeding antenna is a horn type, which can be designed to provide CP [5]. However, these antennas are neither compact nor lightweight. Compact and straightforward feeding antennas that provide CP are desired to reduce size and weight.

In this sense, leaky-wave antennas (LWA) are a good candidate since they can be compact and easy to feed [6]. Planar LWAs that provide CP have been previously presented in the literature, showing the feasibility of offering a compact antenna feed for the reflector [7–9]. These previous examples consist of LWAs designed with PCB manufacturing, mainly based on substrate-integrated waveguide (SIW) or microstrip technologies. Although these designs are sufficiently simple, the radiation occurs from slots etched on the top layer of the SIW or by adding periodic perturbation on one of the sides of the substrate. For this, radiation is mainly directed to the upper semi-space. This limits the area of a reflector that can be illuminated if the feeding is close to it, hence limiting the achievable directivity.

This work proposes a simple and compact CP LWA with conical radiation to illuminate a reflector while the feeder is closed. The proposed structure consists of a coaxial line with a helical slot allowing controlled radiation. Helical antennas have been extensively studied in previous literature to obtain CP quickly. For instance, [10–14] COMPRISES two or more interlaced helical arms. These antennas radiate at the broadside, and no conical beam is generated. Thus, the illuminated reflector area cannot be covered appropriately.

On the other hand, an LWA based on a helix-shaped slot cylindrical waveguide was presented in [15]. A conical beam with CP was generated, but the antenna feeding was

complex, requiring a linear-to-circular polarization (LP-CP) converter [16]. Our proposal presents a much simpler antenna feeding since its coaxial topology makes it compatible with standard SMA connectors if the diameters of the coaxial line are appropriately chosen.

The rest of the manuscript is organized: section 2 presents the proposed structure, explaining the working mechanism and design process. The simulation and measurement results of a manufactured prototype are presented in section 3. Finally, some conclusions are given in section 4.

2. COAXIAL PERIODIC LEAKY WAVE ANTENNA WITH HELICAL SLOT

The proposed LWA consists of a coaxial cable with a helical slot at the outer conductor, as schematically represented in Fig. 1. The slot's helical shape achieves circular polarization, which causes the radiated fields to vary their polarization as the wave propagates inside the coaxial cable.

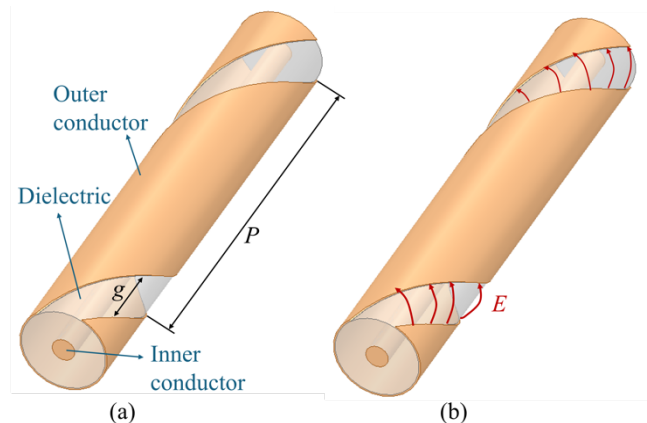


Fig. 1 – Proposed helical-slot coaxial structure. (a) Representation of the unit cell. (b) Radiation mechanism with the E-field lines produced at the slot P – (slot pitch) g – (slot width).

The working mechanism of the antenna can be described as a perturbation of the fundamental TEM mode of the coaxial cable with a slot. Radiation occurs at the slot as there is a phase difference.

In the following section, the development process of uniform and periodic leaky wave antennas will be presented, more precisely, the process used to determine the dimensions

¹ Military Technical Academy “Ferdinand I”, Romania.

² Universidad Politécnica de Cartagena, Spain.

E-mails: alomanalexandru@gmail.com, miguel.poveda@upct.es, ioan.nicolaescu@mta.ro, florin.popescu@mta.ro, laurentiu.buzincu@mta.ro

of the antenna by achieving a variation in the propagation constant of the leaky mode, which in turn provides specified radiation characteristics.

The tapering process described is typical of any leaky-wave antenna with desired illumination control. This method has been applied to antennas in different works published in the literature [17,18]. However, few works have been published where the design process has been automated. In most works, the success of the tapering design depends on the designer's ability to identify a way to control the attenuation constant of the leaky mode without affecting its phase constant or to have control over the changes in the phase constant. The designer must find an antenna dimension that allows for the variation of attenuation constant without affecting the phase constant.

In most cases, this is not possible, and the variation in antenna dimensions affects both parameters. Any phase error the tapering process introduces must be manually corrected by varying the antenna dimensions again. In this way, the antenna dimension design process can become complicated, requiring multiple iterations to achieve the final result.

To analyze a leaky wave structure, dispersion curves must be obtained at the base layer. Dispersion curves describe the relationship between the phase constant and the frequency of the propagating modes within the antenna, providing critical insights into the radiation characteristics and beam steering capabilities.

These curves are essential because they provide insights into how electromagnetic waves propagate along a waveguide or antenna structure, mainly how the phase and attenuation constants vary with frequency and structural dimensions. Dispersion curves also help identify and analyze different modes supported by the structure. For instance, the fundamental and higher-order modes will have different dispersion characteristics, influencing the overall radiation pattern. By examining the dispersion curves, designers can adjust the physical parameters of the antenna, such as slot dimensions, spacing, and periodicity, to achieve the desired radiation characteristics. This includes controlling the beam direction, sidelobe levels, and overall antenna efficiency.

The overall process starts with analyzing the dispersion curves. It continues with the help of a tool developed in MATLAB to obtain a specific attenuation function to achieve a particular radiation pattern. The attenuation function will depend on the illumination type, the antenna length, and the antenna's radiation efficiency. Therefore, the design process begins by inputting the following parameters: operating frequency, antenna length, beam direction, or the normalized phase constant, and antenna efficiency, or the average value of the attenuation constant. Additionally, it is possible to choose between different types of standard illumination functions (uniform, cosine, squared cosine, or triangular). For every kind of illumination, the radiation pattern and the constant function of attenuation will be automatically calculated. Custom illumination functions can also be created, for which the corresponding radiation pattern and the necessary function will be obtained, allowing flexibility beyond the predefined functions.

The following design step transforms the variation of the leaky mode's attenuation constant into a variation of the slot dimensions along the length of the antenna. To do this, it is first necessary to study how the different dimensions of the antenna affect the propagation constant of the leaky mode, which will be used as the radiation source, as evidenced by examining the dispersion curves.

These dispersion analysis results will be stored in a map extension file, which essentially contains a table with the variation of the radiation angle and the normalized attenuation constant concerning the variation of both the period and the width of the helical slot unit. These data will allow the necessary dimensions of the helical slots to be obtained to synthesize the chosen radiation pattern (radiation angle, sidelobe levels, efficiency). The tool responsible for this will combine the information from the dispersion curves to achieve the desired antenna design. Also, contour curves representing the helical slot dimensions needed to achieve a constant value of the radiation angle will be obtained, as well as contour curves where the attenuation constant remains constant.

Interpolation of the results is necessary to obtain sufficiently high-resolution contour curves. Higher resolution yields better contour curves that correspond to exact dimensions. However, higher resolution also means more points to analyze and longer computation times. As the number of interpolated points increases, a more precise curve is obtained. With $\times 10$ interpolation, a continuous curve is produced, containing the exact values of dimensions P and g , capable of indicating constant angles differentiated by a single degree. The tool allows control over interpolation to achieve sufficiently smooth contour curves, eliminating uncertainty due to the lack of analysis points.

Starting from the antenna's feed point and knowing the desired radiation angle, the values for the two structural parameters, P and g , are selected to achieve the appropriate attenuation constant. The cursor is then moved to the starting point of the second slot, where the previous step is repeated. This process continues until the entire length of the antenna is covered.

The final step is to verify that the dimensions of the designed tapered antenna provide the specified radiation pattern initially defined in the design process. Summary of the steps:

1. Starting point: begin at the feed point of the antenna.
2. Parameter selection: based on the desired radiation angle, choose values for P and g to obtain the suitable attenuation constant.
3. Slot progression: move to the starting point of the next slot and repeat the parameter selection process. Adjust P and g as needed to maintain the desired radiation characteristics.
4. Iterative process: continue this process iteratively for each slot along the length of the antenna, ensuring the structure aligns with the desired attenuation function.
5. Full antenna length: repeat the above steps until the entire length of the antenna length is covered.
6. Verification: verify that the tapered antenna design provides the radiation pattern specified at the beginning of the design process. This includes checking the overall radiation characteristics to ensure they meet the design requirements.

3. RESULTS

The proposed structure has been designed, simulated, manufactured, and tested. A picture of the prototype is presented in Fig. 2, along with the simulated HFSS model for comparison. As can be seen, a handmade manufacturing process has been followed for quick validation. For this, a standard semi-rigid coaxial cable with SMA connectors attached to it was peeled off by removing the outer mesh, and the conductive copper tape was used to create the slotted outer conductor.

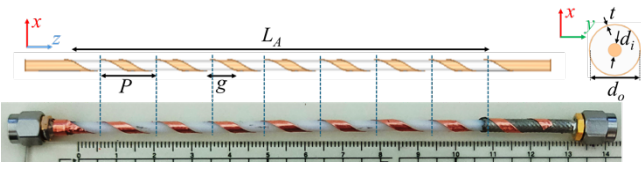


Fig. 2 – Picture of the manufactured prototype with dimensions $L_A=10.8$ cm, $P=1.42$ cm, $g=0.9$ cm, $d_i=0.8$ cm, $d_o=2.98$ cm, $t=0.1$ mm.

Dimensions of the structure are given in the caption of Fig. 2 with dielectric constant $\epsilon_r = 2.25$. The antenna is fed by one of the ports, and the other one is connected to a matched load to absorb the remaining power that has not been radiated along the antenna.

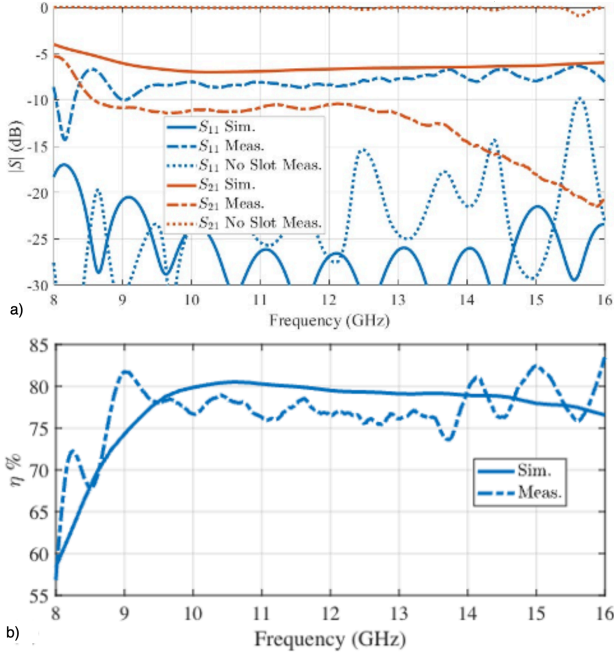


Fig. 3 – Simulated and measured S parameters and efficiency η of the manufactured prototype. (a) S parameters. (b) Efficiency η .

First, the S parameters are presented in Fig. 3(a), with the simulated ones in a solid line and the measured ones in a dashed line. The simulation shows good matching S_{11} , which is well below -10 dB in all the frequency bands from 8 GHz to 16 GHz. On the other side, measurement S_{11} is degraded. This is mainly attributed to handmade manufacturing since inaccuracies can be significant, especially in peeling off the cable and wrapping the copper tape around the dielectric material. When additional measurements were conducted with the cable entirely covered by copper tape, the S_{11} values fell between those obtained from the simulations and those from the slotted cable measurements. This outcome demonstrates that even adding a non-slotted copper band over the dielectric increases reflection. S_{21} was also measured to evaluate the amount of non-radiated power. In simulation, it is around -7 dB, while in measurement, it is below -10 dB in almost all the frequency bands. This reduction in the S_{21} is directly related to the increase S_{11} since less power enters the antenna and, hence, less power reaches the opposite port. With this, the antenna radiation efficiency can be evaluated as follows:

$$\eta = 1 - |S_{11}|^2 - |S_{21}|^2 \quad (1)$$

Equation (1) considers the ratio between the power entering the antenna and the radiated power. This is represented in Fig. 3(b). It can be observed that the measured efficiency is

very similar to the simulated one with a value above 75 % in almost all the frequency range. Thus, although the S_{11} is degraded, a similar ratio of power is radiated. It must be highlighted that efficiency remains significantly constant, meaning that the pical open stop-band (OSB) effect consists of the efficiency degradation when the antenna radiates around a broadside direction ($\theta_R = 0^\circ$) is strongly reduced, as shown hereunder. This is due to the antenna's particular topology, which constantly radiates along a uniform slot despite working as a periodic LWA because of the helical shape of the slot.

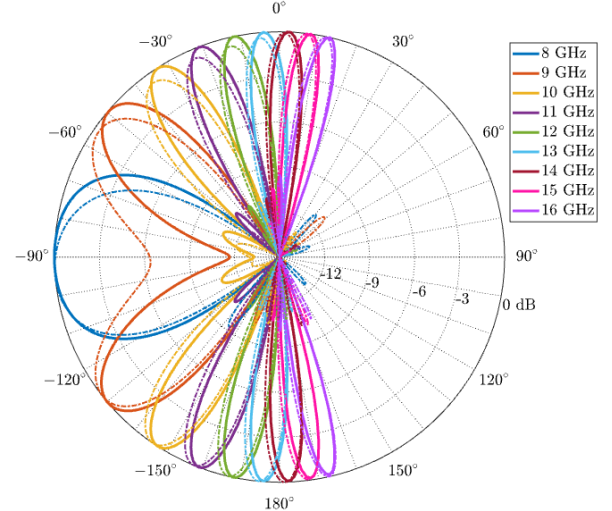


Fig. 4 – Simulated (solid) and measured (dashed) LHCP radiation pattern of the manufactured prototype at different frequencies in the xz-plane.

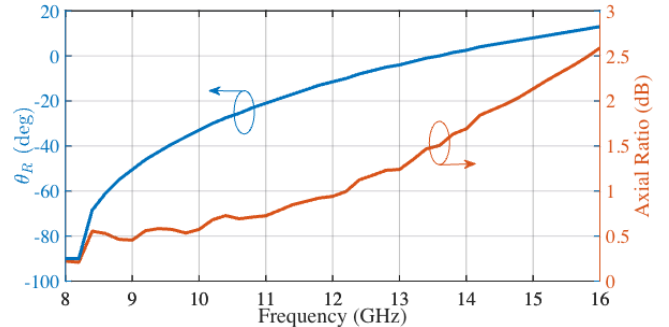


Fig. 5 – Beam direction θ_R and Axial Ratio of the manufactured prototype.

The radiation patterns at different frequencies are plotted in Fig. 4. Again, the solid line represents the simulated results, while the dashed line represents the measurements. It is seen that measurements agree with the simulated results, showing the expected performance of the antenna. Due to manufacturing errors, the measured radiation patterns slightly shifted from 8 GHz to $\theta_R = 12^\circ$ 16 GHz. This confirms the OSB cancellation since efficiency is kept constant while the beam is scanned around the broadside in frequencies around 14 GHz. The change of the beam direction with the frequency is represented in Fig. 4, showing the typical trend in periodic LWAs with the beam direction increasing with frequency and with faster scanning at the low-frequency band. On the other side, to evaluate the CP performance, the simulated axial ratio (AR) is also represented in Fig. 5. Along all the frequency bands, the AR is below 3 dB, confirming the desired CP radiation from the LWA.

4. CONCLUSION

This study presents a novel design of a coaxial-line-based helical leaky-wave antenna that efficiently achieves circular

polarization through an innovative helical slot structure etched on the outer conductor of a coaxial cable. The research demonstrates that this antenna can maintain high radiation efficiency, exceeding 75 % across the entire operational frequency band of 8 GHz to 16 GHz, while providing continuous beam scanning from -90° to 12° . The design mitigates the open stop-band effect, which typically hampers radiation efficiency around broadside angles. This is achieved by ensuring continuous radiation along the uniform helical slot, making the antenna suitable for high-frequency applications where consistent performance is critical.

The simulation and experimental measurement results confirm the antenna's capability to deliver robust CP performance with an axial ratio consistently below 3 dB. The agreement between the simulated and measured results underscores the reliability of the design. However, slight discrepancies are noted due to manufacturing tolerances, particularly in the handmade process of creating the helical slots.

The proposed LWA design holds significant promise for satellite communication systems, where compact, lightweight, and efficient CP antennas are essential. The simplicity of the coaxial topology, combined with the helical slot design, allows for compatibility with standard SMA connectors, facilitating easier integration into existing systems.

One of the primary challenges encountered in this study was the manual manufacturing process, which introduced slight deviations in performance metrics such as the S-parameters. These discrepancies highlight the need for more refined and precise manufacturing techniques to ensure consistent performance across multiple prototypes. Additionally, while the current design achieves good results, the complexity of the tapering process, particularly in adjusting the antenna dimensions to control the propagation constant without affecting the phase constant, remains a potential area for further optimization.

CREDIT AUTHORSHIP CONTRIBUTION STATEMENT

Alexandru Aloman: Responsible for determining the dispersion curves, which formed the basis of the antenna model subjected to measurements. Conducted the mathematical and numerical analysis required to extract the propagation parameters, ensuring the model's accuracy. Developed the MATLAB software tool to obtain the specific attenuation function essential in generating the optimal radiation model. He played a key role in interpreting the received data and correlating it with experimental results.

Ioan Nicolaescu: Proposed the general analysis methodology and conducted the initial theoretical study, enabling the correct derivation of the dispersion curves. Contributed to formulating the working hypotheses and defining the boundary conditions essential for the modeling process. Analyzed the impact of different structural configurations on the antenna's performance and provided recommendations for design optimization. Ensured the theoretical coherence of the approach and supervised the validation of the model through analytical methods.

Florin Popescu: Suggested using the helical shape of the feeder to achieve circular polarization, a crucial factor in improving the illumination of the reflector. Conducted comparative studies to highlight the advantages of this configuration over conventional alternatives and contributed to defining structural details, including material selection and optimizing component geometry. Also participated in numerical simulations to validate the proposed solution before fabrication.

Miguel Poveda: Managed the fabrication process of the antenna prototype, ensuring compliance with theoretical and structural specifications. Performed experimental measurements in the laboratory, using specialized equipment to characterize the antenna's performance. Analyzed experimental data to identify potential deviations from simulations and

proposed adjustments to enhance the design. Closely collaborated with the other authors to correlate experimental findings with theoretical predictions.

Laurentiu Buzincu: Focused on interpreting and analyzing the obtained results, conducting detailed comparisons between theoretical and experimental values. Identified possible sources of error and adjusted the mathematical model to better align with practical data. Drafted the final comparative analysis, emphasizing the strengths and limitations of the proposed solution. He also played a key role in synthesizing conclusions and preparing the material for publication.

Received on 19 September 2024

REFERENCES

1. C.A. Balanis, *Antenna Theory: Analysis and Design*, Wiley, 4th ed. (2015).
2. K. Woellert, P. Ehrenfreund, A.J. Ricco, H. Hertzfeld, *Cubesats: cost-effective science and technology platforms for emerging and developing nations*, Adv. Space Res., **47**, 4, pp. 663–684 (2011).
3. N. Chahat, E. Decrossas, D. Gonzalez-Ovejero, O. Yurduseven, M.J. Radway, R.E. Hodges, P. Estabrook, J.D. Baker, D.J. Bell, T.A. Cwik, G. Chattopadhyay, *Advanced cubesat antennas for deep space and earth science missions: A review*, IEEE Antennas Propag. Magaz., **61**, 5, pp. 37–46 (2019).
4. M.D. Samsuzzama, Mohammad Tariqul Islam, Mandeep Jit Singh, *Ceramic material based multiband patch antenna for satellite applications*, Rev. Roum. Sci. Techn. – Électrotechn. et Énerg., **59**, 1, p. 77–85 (2014).
5. G. Mishra, S.K. Sharma, J.-C.S. Chieh, *A circular polarized feed horn with inbuilt polarizer for offset reflector antenna for w-band cubesat applications*, IEEE Transactions on Antennas and Propagation, **67**, 3, pp. 1904–1909 (2019).
6. A.A. Oliner, D.R. Jackson, *Leaky-wave antennas*, Antenna Engineering Handbook, ch. 11, New York, NY, USA: McGraw-Hill (2007).
7. X. Li, J. Wang, G. Goussetis, L. Wang, *Circularly polarized high gain leaky-wave antenna for CubeSat communication*, IEEE Trans. Antennas Propag., **70**, 9, pp. 7612–7624 (2022).
8. M.M. Sabahi, A.A. Heidari, M. Movahhedi, *A compact CRLH circularly polarized leaky-wave antenna based on substrate-integrated waveguide*, IEEE Trans. Antennas Propag., **66**, 9, pp. 4407–4414 (2018).
9. G. Mishra, S.K. Sharma, J.-C.S. Chieh, *A high gain series-fed circularly polarized traveling-wave antenna at W-band using a new butterfly radiating element*, IEEE Trans. Antennas Propag., **68**, 12, pp. 7947–7957 (2020).
10. H. Wheeler, *A helical antenna for circular polarization*, IRE, **35**, 12, pp. 1484–1488 (1947).
11. A. Adams, R. Greenough, R. Wallenberg, A. Mendelovicz, C. Lumjiak, *The quadrifilar helix antenna*, IEEE Trans. Antennas Propag., **22**, 2, pp. 173–178 (1974).
12. Y.-S. Wang, S.-J. Chung, *A miniature quadrifilar helix antenna for global positioning satellite reception*, IEEE Trans. Antennas Propag., **57**, 12, pp. 3746–3751 (2009).
13. J. Costantine, Y. Tawk, I. Maqueda, M. Sakovsky, G. Olson, S. Pellegrino, C.G. Christodoulou, *UHF deployable helical antennas for cubesats*, IEEE Trans. Antennas Propag., **64**, 9, pp. 3752–3759 (2016).
14. Y. Tawk, J. Costantine, *A polarization reconfigurable 3D printed dual integrated quadrifilar helix antenna array embedded within a cylindrical dielectric mesh*, IEEE Trans. Antennas Propag., **71**, 1, pp. 309–317 (2023).
15. Y. Liu, M. Li, K. Song, D. Hu, H. Liu, X. Zhao, S. Zhang, M. Navarro-Cia, *Leaky-wave antenna with switchable omnidirectional conical radiation via polarization handedness*, IEEE Trans. Antennas Propag., **68**, 3, pp. 1282–1288 (2020).
16. I. Nicolaescu, P. van Genderen, Archimedean, *Spiral antenna calibration procedures to increase the down range resolution of an SFCW radar*, International Journal on Antennas and Propagation, **1**, pp. 1–7 (2008).
17. A. Alexandru, N.V. Petrescu, I.V. Grecu, J.L.G. Tomero, *Analysis and design of line-source slotted-coaxial feeders for conical reflectors antennas*, International Conference on Communications (COMM) (2018).
18. A. Alexandru, M.P. Garcia, I.V. Grecu, J. Luis, G. Tornero, *Analysis and design of line-source slotted-coaxial feeders for conical reflectors antennas*, International Conference on Communications (COMM) (2022).